

Behaviour of propagator and quark confinement

Vladimir Šauli^{1,2}

¹*CFTP and Dept. of Phys., IST, Av. Rovisco Pais, 1049-001 Lisbon, Portugal*

²*Dept. of Theor. Phys., INP, Řež near Prague, AVČR*

The propagator of confined quarks is calculated for timelike momenta by transforming Minkowski Greens functions to the Temporal Euclidean space. Based on the framework of the Schwinger-Dyson equations the QCD quark propagator is obtained in two approximations which differ by assuming behaviour of gluon propagator. In both studied cases we get universal result for the light quarks: The quark mass function becomes complex below expected perturbative threshold, the obtained absolute value of the infrared mass is $M \simeq \Lambda_{QCD}$ with the infrared phase $\simeq \frac{\pi}{2}$. Permanent confinement of quarks is maintained by generation of the complex mass function which prevents a real pole in the propagator. We will show that timelike dynamical Chiral Symmetry Breaking (CSB) solution is approximately, but non-trivially determined by the solution of gap equation in the standard Euclidean space.

PACS numbers:

I. INTRODUCTION

Quark confinement in Quantum Chromodynamics (QCD) is theoretically unsolved phenomenon of longstanding interest [2, 3, 4, 5, 6, 7, 8, 9]. QCD as the strong coupling theory is not easily tractable, thus the confinement of colored object has been questioned in various indirect ways. Considering static infinitely heavy color sources the linearly rising potential was predicted and observed by simulation on the Euclidean lattice [10].

The alternative to the lattice theory is the continuous framework of the Schwinger-Dyson equations (SDEs) which in principle could provide a unique powerful tool for the nonperturbative QCD study (for a reviews see [11, 12, 13, 14]). While it is naturally expected that the SDEs Euclidean formulation should approximately corresponds to the continuum limit of lattice data whenever they are available, however the real advantage of SDEs approach is the possibility to explore directly all Minkowski space. To that point, based on the spectral representation, the problem has been formulated in Minkowski space and the results have been actually obtained for a weak or a medium coupling quantum field theory (for a review see [15]). Actually for several cases of toy models the true equivalence between Minkowski Greens functions evaluated at spacelike momenta and the calculated in the Euclidean space from the beginning has been explicitly checked by the numerical solutions. For gluodynamics (QCD without quarks) the problem was formulated by using covariant Gauge/Pinch technique method time ago [16], however never solved in Minkowski space in practise. Recently, we have no idea how much the analytical assumptions are justified for gluons, however we have no doubts that the usual analyticity is too strong assumption for the quark propagator [17]. To get chiral symmetry breaking with an analytical quark propagator, i.e. which has a standard branch cut on the positive p^2 semi-axis, is very likely impossible - the quark propagator doesn't satisfy Lehmann representation.

Direct solution of SDEs for strong coupling theory system in Minkowski space is still very complicated task and as we discuss above it requires an additional assumptions. To get rid of part of the mentioned weaknesses (e.g. assumption of the spectral representation) the SDEs has been recently formulated in Temporal Euclidean (ET) space [18, 19], providing us with the solution for Greens function for the timelike, but Euclidean momenta. In this case we have the Euclidean metric $p_{ET}^2 = \sum_{i=1}^4 p_i^2$

$$p = (p_1, p_2, p_3, p_4)^{[ET]} = (p_0, -ip_1, -ip_2, -ip_3)^{[M]}, \quad (1.1)$$

where Eq. (1.1) explicitly shows the prescription between the components of Temporal Euclidean -ET- and Minkowski -M- fourvector. Recall here, the prescription for the measure $d^4 p_M = id_{ET}^4$ with real $\pm\infty$ boundaries in a momentum loop integrals. Likewise for the standard -time component- Wick rotation [20] the equivalence between ET space and Minkowski subspace is the assumption. Here, it is noteworthy that it was recently proved in [19] that the ladder approximation of Minkowski QED2+1 is exactly equivalent to the formulation of the problem in ET space.

If the full fermion propagator has no mass singularity in the timelike region, it can never be on-shell and thus never observed as a free particle [21, 23, 24, 29]. In our solution the imaginary part of the mass function is automatically generated for a coupling strong enough. In the paper [18] such result was firstly obtained for explicitly massive quark with bare current mass $m \sim \Lambda_{QCD}$. At that time the authors of [18] were not able to obtain the results for an arbitrary quark mass because of numerical obstacles accompanying their specific model. Therefore the main purpose of our paper is to present a models and techniques that exhibit good numerical stability for all quarks flavors, e.g. for the light u, d quarks and hypothetical massless case as well. We will show that the light quark mass is the complex

functions with relatively tiny real parts in the infrared. The infrared complex phase is approximately given by the ratio of the current and the infrared (constituent) quark mass. Quite interestingly, described complexification is universal and it doesn't depend on the details of the interaction kernel. As we will show explicitly the qualitative feature of observed complexification is independent on the (un)presence of (pole) type singularity in the kernel.

As an another interesting model possibility we decreased the infrared running coupling and we study confinement and CBS phenomena near the phase transition, where generated mass is particularly small when compare to the scale of confinement, $M \ll \Lambda$. The observed results are relevant for the Technicolor models, eg. to walking Technicolors wherein large number of fermions makes the strong coupling softer in the infrared (originally these models have been developed to avoid flavor changing neutral current, however they have their own interest).

After the introduction of the models details in the next Section the numerical results are presented in the Section III. In this section we discuss the relation with the standard Euclidean solution. In the Section IV we summarize and conclude.

II. THE MODELS- DRESSED LADDER APPROXIMATION OF QUARK SDE

The quark gap equation we solved is the rainbow ladder approximation of the full quark SDE. In this Section we describe the details of the models employed here. In the ladder approximation the quark SDE reads

$$\begin{aligned} S^{-1}(p) &= S_0^{-1}(p) - \Sigma(p), \\ \Sigma(p) &= iC_A g^2 \int \frac{d^4 q}{(2\pi)^4} \gamma_\alpha G^{\alpha\beta}(p-q) S(q) \gamma_\beta, \end{aligned} \quad (2.1)$$

where the full gluon-quark-antiquark vertex of the exact SDE has been replaced by the standard four dimensional Dirac matrix, which obey anticomutation relation $\{\gamma_\mu, \gamma_\nu\} = 2g_{\mu\nu}$ (we use the Minkowski metric $g_{\mu\nu} = \text{diag}(1, -1, -1, -1)$) and where $C_A = T_a T_a = 4/3$ for $SU(3)$ group and $G^{\alpha\beta}$ is the gluon propagator. The quark propagator S can be parametrized by two scalar functions conventionally like

$$S(p) = S_v(p) \not{p} + S_s(p) = \frac{1}{\not{p}A(p) - B(p)}. \quad (2.2)$$

The renormgroup invariant mass function is defined as $M = B/A$, the physical mass M_p could be identified by the pole position of S i.e. by the solution $M^2(M_p^2) = M_p^2$ in unconfining theory.

We assume these functions are complex, therefore it is convenient to parametrized them in the following way

$$\begin{aligned} S_s(x) &= \frac{B(k)}{A^2(k)k^2 - B^2(k)} \\ &= \frac{R_B [(R_A^2 - \Gamma_A^2)k^2 - R_B^2 - \Gamma_B^2] + 2R_A \Gamma_B \Gamma_A k^2}{D} \\ &\quad + i \frac{\Gamma_B [(R_A^2 - \Gamma_A^2)k^2 + R_B^2 + \Gamma_B^2] - 2R_B R_A \Gamma_A k^2}{D}, \end{aligned} \quad (2.3)$$

$$\begin{aligned} S_v(k) &= \frac{A(k)}{A^2(k)k^2 - B^2(k)} \\ &= \frac{R_A [(R_A^2 + \Gamma_A^2)k^2 - R_B^2 + \Gamma_B^2] - 2R_B \Gamma_A \Gamma_B}{D} \\ &\quad + i \frac{\Gamma_A [-(R_A^2 + \Gamma_A^2)k^2 - R_B^2 + \Gamma_B^2] + 2R_A R_B \Gamma_B}{D}, \end{aligned} \quad (2.4)$$

where R_A, R_B (Γ_A, Γ_B) are the real (imaginary) parts of the functions A, B and the denominator D reads

$$D = ([R_A^2 - \Gamma_A^2]k^2 - [R_B^2 - \Gamma_B^2])^2 + 4(\Gamma_A R_A - \Gamma_B B)^2. \quad (2.5)$$

The last missing ingredient which completes our considered gap equation is the gluon propagator. With the exception of the large timelike momenta $p^2 > \Lambda_{QCD}^2$, where the effective coupling is small and the result is available by the analytical continuation of the Euclidean perturbation QCD, gluon propagator is basically unknown function for timelike momenta. Most of the last decades nonperturbative studies were devoted to the quark SDE in Landau

gauge, thus for a possible comparison we will work in this gauge as well. The Landau gauge Gluon propagator is completely transverse

$$G_{\mu\nu} = \frac{-g_{\mu\nu} + (1 - \xi) \frac{k_\mu k_\nu}{k^2}}{k^2} G(k^2), \quad (2.6)$$

and is fully determined by the gluon form factor G which we will model as it is described below.

A. Model I.

The model I. is based on a simple generalization of the perturbative one loop result for the gluon form factor. For this purpose we consider the kernel (in fact the effective product of gluon propagator and γ_μ part of the vertex function) such that it has a standard single pole and the the function G is taken as

$$\frac{g^2}{4\pi} G(q^2) = \frac{4\pi/\beta}{\frac{1}{2} \ln \left[e + \left(\frac{q^2}{\Lambda^2} \right)^2 \right]} \quad (2.7)$$

where β in (2.11) represents the beta function coefficient, for which we take $4\pi/\beta = 1$ (recall, $4\pi/\beta = 1.396$ for three active quarks in perturbative QCD). The prefactor is adjusted in a way that Eq. (2.7) behaves as QCD running coupling at ultraviolet, i.e.

$$\frac{g^2}{4\pi} G(|q^2| \gg \Lambda_{QCD}^2) \simeq \frac{4\pi/\beta}{\ln(\pm q^2/\Lambda_{QCD}^2)}, \quad (2.8)$$

where \pm stands for timelike or spacelike q^2 respectively. In the infrared effective running coupling defined as $g^2 G(0)/(4\pi) = 2$, thus the function G is large enough to generate QCD typical CSB and and it provides confinement of quarks for any flavor as well.

B. Model II.

The second model we use represents a slight modification of the one already considered in [18]. In this case, the gluon propagator is expressed through the following spectral representation:

$$\frac{g^2}{4\pi} \frac{G(q^2)}{q^2} = \int_0^\infty d\nu \frac{\rho_g(\nu, \Lambda_{QCD})}{q^2 - \nu}, \quad (2.9)$$

The function ρ_g we consider here is a regular smooth function, ensuring thus there is no pole in the gluon propagator. The main difference comparing to [18] is that we drop out the usual Feynman $i\varepsilon$ prescription so the principal value integration is understood for the timelike momenta in (2.9). As far as we are not considering the feedback of complex quark loop the gluon propagator is clearly real for all Minkowski q^2 .

In principle the weight function ρ_g can be obtain by solving the gluon gap equation as suggested in [16] and further considered recently in [25, 26, 27] (up to the changes followed from the $i\varepsilon$ absence).

Following the arguments presented in [27], it seems that gauge invariant gluon propagator is not "strong" enough to trigger CSB. Very likely, the next leading vertex correction must enforce the kernel to get the expected picture of CSB and confinement. To that point we simplify and make a phenomenological choice of the function ρ_g which provide the desired solution.

The function we actually use in our numerical study reads

$$\rho_g(x) = \frac{\alpha(x)}{\alpha(0)} \frac{\rho_\alpha(x)}{x + 0.1\Lambda^2} \quad (2.10)$$

where the function $\alpha(x)$ is calculated through

$$\begin{aligned} \rho_\alpha(x) &= \frac{4\pi/\beta}{\pi^2 - \ln^2(x/\Lambda_{QCD}^2)}, \\ \alpha(x) &= P. \int_0^\infty d\nu \frac{\rho_\alpha(\nu)}{x - \nu}, \end{aligned} \quad (2.11)$$

where symbol P stands for Cauchy principal value integration. For the reader familiar with our previous paper on Temporal Euclidean QCD, now gluon form factor is twice weaker there is factor 2 omitted in (2.11), further the infrared cutoff $0.1\Lambda^2$ is introduced in (2.10) in order to have finite and smoothed gluon propagator G/q^2 in the infrared. Evaluating the integral one can see that for a very large momenta the gluon propagator is softened by the power of log, i.e.

$$\frac{g^2}{4\pi}G(|q^2| \gg \Lambda_{QCD}^2) \simeq \frac{4\pi/\beta}{2\ln^2(\pm q^2/\Lambda_{QCD}^2)} \quad (2.12)$$

(this fact has been overlooked in [18]). This affects the UV tail of quark mass function, but is quite unimportant for the low the energy behaviour of the quark mass function $M(0)$.

III. SOLUTION OF THE GAP EQUATION

A. QCD light quarks

The quark gap equation have been solved numerically by the standard method of iterations. The Gaussian numerical integrator with 600 mesh points was used for all the numerical integrations. The angular integration has been performed analytically in the model II, thus we only numerically integrate over the auxiliary variable ν . To avoid numerical noise, large density of the mesh points for $q^2 \simeq \Lambda$, $\nu \simeq \Lambda$ was used in the Model II. Furthermore, in order to achieve numerically stability during the run of iteration process, we gradually decreased current quark mass to reach the massless limit. The model I is completely stable, whilst there is a small numerical noise for a low q^2 in the model II.

Actually, what we have solved was the system of four real equations for the functions $R_A, \Gamma_A, R_B, \Gamma_B$. These have been obtained by standard trace projections (of Dirac matrices), what leads to the coupled system of two equations for the functions A, B in the first step.. After performing the 3d-space Wick rotation, we get the expressions in the Temporal Euclidean space. Further using Eqs. (2.4) we arrive to the equations for the imaginary and real parts – Cartesian complex coordinates of A, B – the functions $R_A, \Gamma_A, R_B, \Gamma_B$. Procedure is very straightforward and we do not list the result here, however the reader can find the equation for B in Section IIIC, where the properties of the solution are discussed.

As in the case of perturbation theory, the equations contain UV divergences which require renormalization. The chiral limit is considered for both the models. The only renormalization function A is renormalized, the function B is finite in this case. In the case of light quarks we assume that the ultraviolet timelike behaviour is similar to the spacelike one, hence we set a small real renormalized quark mass $M(\mu^2) \simeq \Lambda_{QCD}/100$ for a very large timelike μ^2 . In this paper all dimensionfull quantities are scaled by Λ_{QCD} , having a typical value for $\Lambda_{QCD} = 250 - 350 GeV$ we set a few MeV light quarks at $200 - 300 GeV$ (a given mesh point is chosen for convenience, thus the corresponding value of the renormalization point is $\mu = 920.3\Lambda_{QCD}$ for presented solution here). In this case we subtract the real parts of functions A, B setting the renormalized values $ReA = 1, ReB = \Lambda_{QCD}/100$ at the renormalization scale μ . As in [18], the imaginary part is expected to be finite and therefore not subtracted. This procedure clearly maintains the hermicity of the classical Lagrangian.

Having the numerical solutions we calculated the magnitude and the mass function phase defined as $M = B/A, \phi = |M|e^{i\phi_M}$. The appropriate results are presented in Fig.1-3. Renormalization wave function A for our models is shown in Fig.4. It is approximately real everywhere, the imaginary part portion obtained $\simeq 10^{-8}$ is smaller then estimated numerical error. There is no remarkable difference between the solution of A for u, d quarks and for the exact chiral limit. In the case of model II these two lines are not distinguishable. The absolute values of the mass functions are shown in Fig.1. In the case of the model II, the function $|M|$ shows up the maximum at $\simeq 2\Lambda_{QCD}$ where it also cuts the linear function of p . This details are better seen in the Fig.2 where we show the infrared details with linear axis scaling.

As a bonus of our CSB solution we get the pion Bethe-Salpeter wave function $\chi(P = 0, p) \simeq B(p)$ [11], which is the Goldstone boson manifestation of broken chiral symmetry here.

Not similarly to previously studied confining theory QED2+1 [19], where a quite tiny imaginary part preserves regularity of the time axis propagator, here a huge dynamical generation of imaginary part mass function M is observed. For pure CSB ($m = 0$) case the observed generated mass is purely imaginary and the same is approximately valid for the infrared mass when small explicit breaking is considered. In both cases, the imaginary part vanish at high p . The phase ϕ of the running quark mass function for the models I and II respectively is shown in Fig 1. The chiral limits are always $\phi = \pi/2$ for both models and hence not displayed. Increasing a current quark mass, the phase is decreasing (rather say its absolute value, there are possibly more than one solution for a quark light enough [28]),

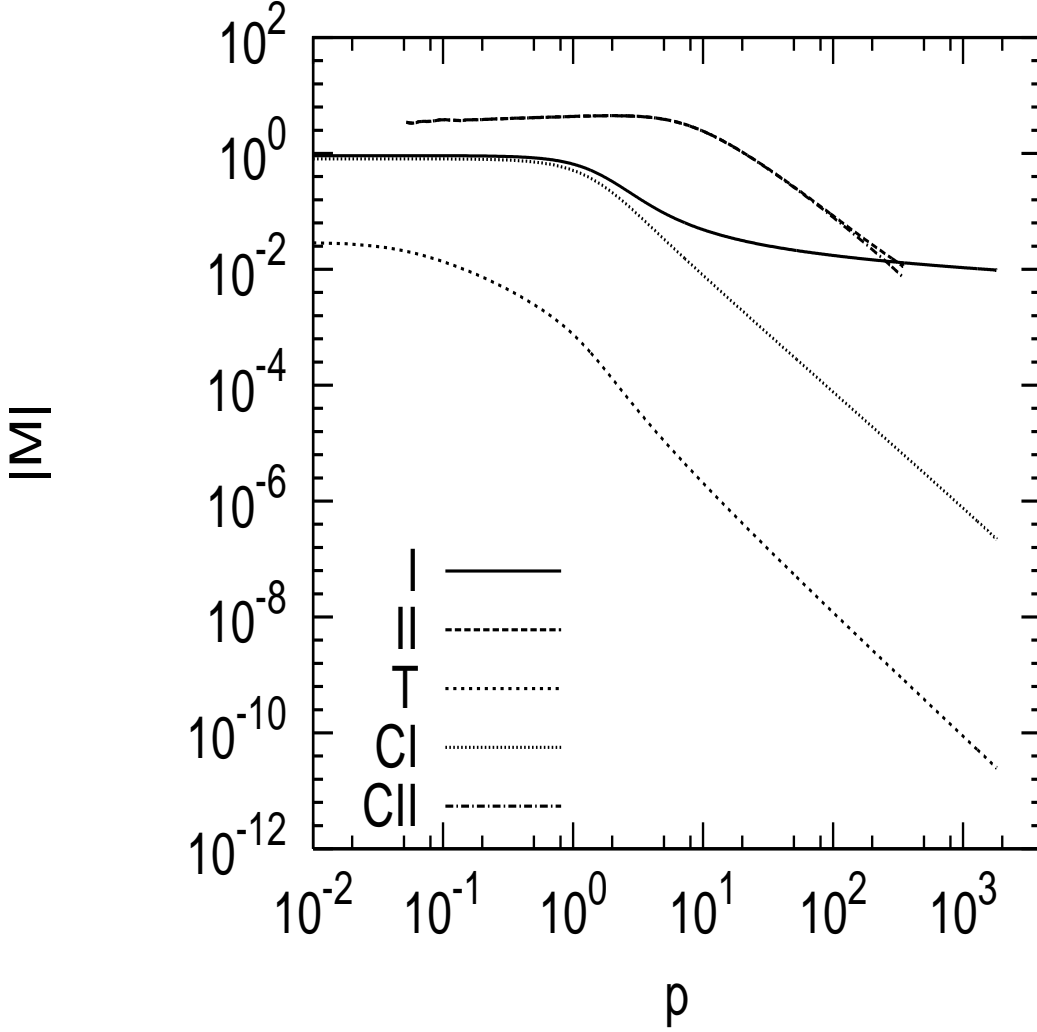


FIG. 1: Magnitude $|M|$ of the running quark mass function $M = |M|e^{i\phi}$ for modeled QCD I,II, its chiral limit CI,CII. The "Walking Technicolor" T solution is added for for the comparison, scale is $\Lambda_{QCD} = 1$ (and $\Lambda_{Tech.} = 1$ is set up in this case as well)

however from a certain value of the quark current mass it does not disappear at its stay constant from some p . A more complete study on heavy quark confinement will be published elsewhere. Further discussion of the solution, after the following Technicolor digression, will follow in the section III C.

B. Criticality in large N_f QCD, walking Technicolor and views in ET space

QCD is an example of non-Abelian gauge theory with small -two or three- approximately massless fermions. If the number of massless fermions is larger, but the asymptotic freedom is still preserved at some high scale, the theory is conformal in the infrared, which have been already suggested by the analysis based on two loop beta function [30, 31] and analyzed for variety of gauge theories (see [32] and references therein). Non-Abelian quantum field theory with possibly large but yet supercritical number of (classically) massless fermion appears as an alternative candidate for electroweak symmetry breaking [33, 34, 35]. Typically in these "walking Technicolor" models, the number of fermions set up the scale Λ_T which characterize running of the effective coupling, which is much larger then fermion mass generation $M(0) < \Lambda_T$. In other words, the conformal infrared nontrivial coupling is adjusted a few percentage above its critical level, say defined at zero momenta $\alpha_c(0) = g^2/(4\pi)$, where g is a gauge coupling. In these theories the coupling is "slowly walking" with momentum in the infrared $p < \Lambda$ where it ensures CSB. The CSB and Technihadrons spectrum in these models have been studied in [36, 37, 38, 39].

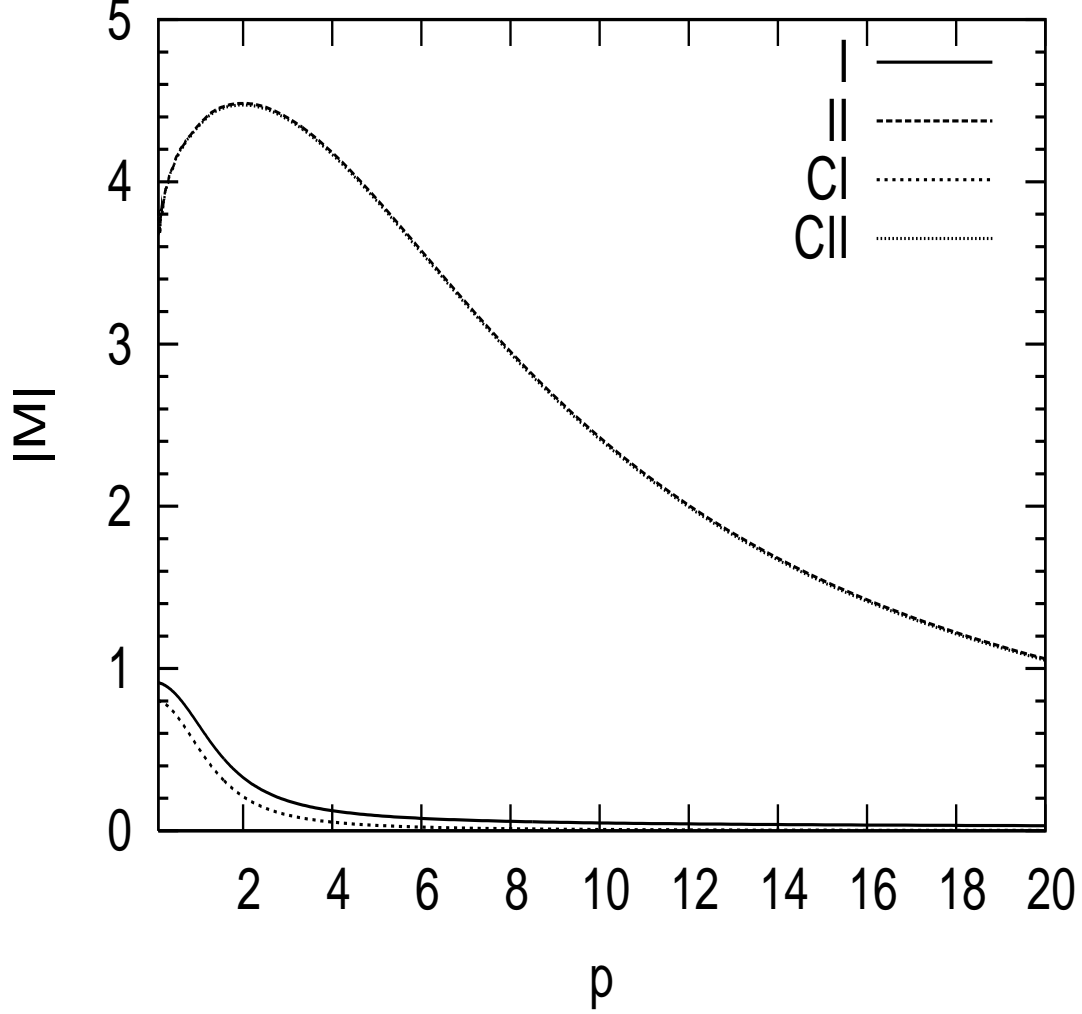


FIG. 2: I infrared behaviour of the functions M as they are in the Fig. 1, but in with linear axis. The solution for large N_f is omitted here.

Identification of the critical number of the flavors for given theory requires nonperturbative knowledge of infrared behaviour of the running gauge coupling. For $SU(3)$ gauge group a recent estimate based on the lattice simulations gives $8 < N_f^c < 12$ [40, 41]. To model the quark gap equation for large N_f we adjust the infrared gluon form factor to be close to minimal strength necessary to trigger CSB. It is achieved by taking the constant $\beta = 1/3$ of the model I , which model is particularly suited for this purpose. We have found the critical couplings are the same in the Standard Euclidean formulation and the one obtained in the Temporal Euclidean space. The obtained CSB solution in ET space solution is confining one, the mass function B is purely imaginary in his case. The renormalization wave function A remains real receiving expected smaller corrections than in the case of QCD.

Decreasing infrared coupling furthermore we obtain only trivial solution for the function B .

C. Further observation

Let as consider the gap equation in more details. As the consequence of our special model I we get with astonishing accuracy the following relation

$$\begin{aligned} A(p^2 > 0) &= A^{ET}(p^2) = A^E(p^2) = A(p^2 < 0) \\ B(p^2 > 0) &= B^{ET}(p^2) = iB^E(p^2) = iB(p^2 < 0). \end{aligned} \quad (3.1)$$

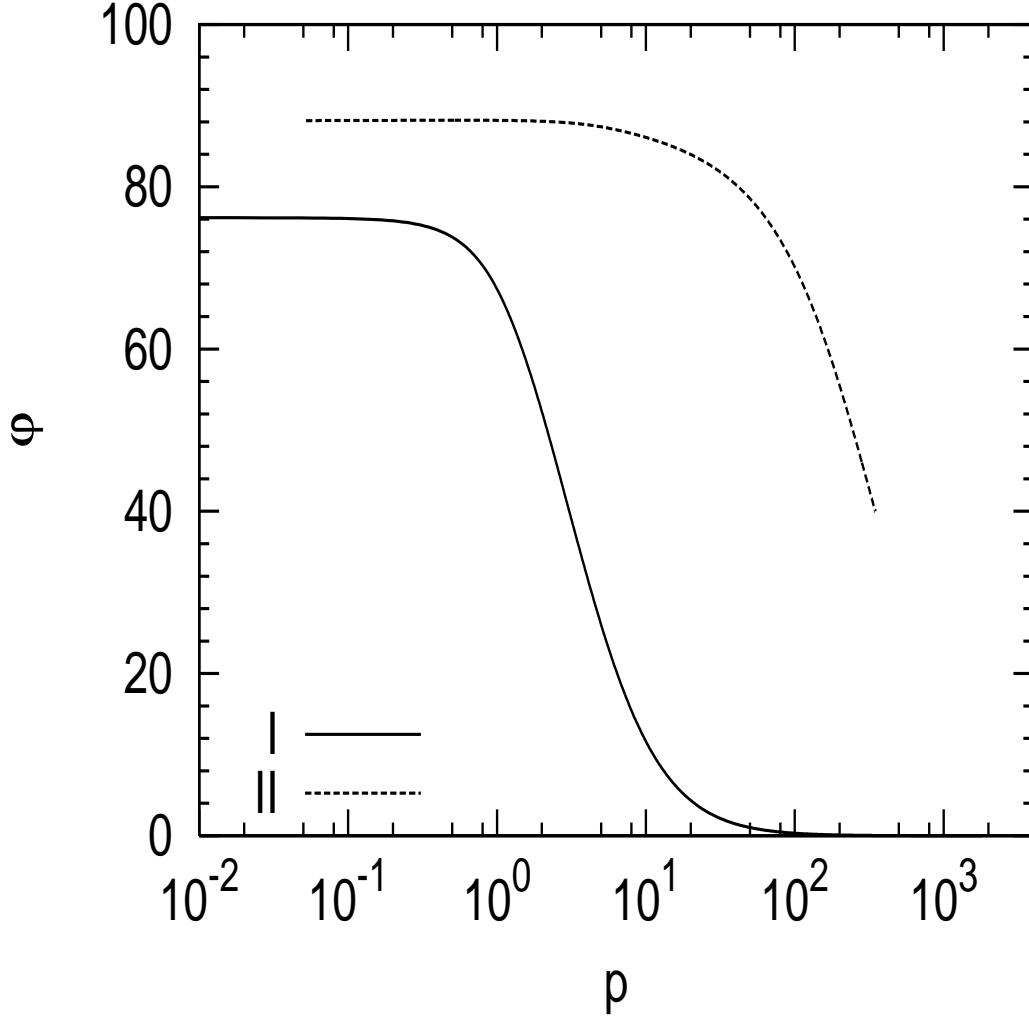


FIG. 3: Phase ϕ of the running quark mass function $M = |M|e^{i\phi}$ for the models I and II respectively, axis momentum is in the units of Λ_{QCD} .

between spacelike and timelike solution. The first is obtained in standard Euclidean formulation, while the second in ET space for pure CSB, $m = 0$. A small current mass leads to a small deviation only.

The exact symmetry (3.1) is directly visible by the inspection of the SDE for B which in ET space reads

$$B(x) = \frac{4}{\pi} \int_0^\infty dy \frac{B(y)}{A^2(y)y - B^2(y)} \int_{-1}^1 dz V(x, y, z)$$

$$V(x, y, z) = \frac{y\sqrt{1-z^2}}{q^2 \log(e + q^4/\Lambda^4)}, \quad (3.2)$$

where here $q^2 = x + y - 2\sqrt{xyz}$.

For the standard (spacelike) Euclidean formulation the gap equation reads

$$B(x) = \frac{4}{\pi} \int_0^\infty dy \frac{B(y)}{A^2(y)y + B^2(y)} \int_{-1}^1 dz V(x, y, z). \quad (3.3)$$

The symmetry 3.1 is manifest. In other words: for the Minkowski kernel which is even with respect of argument of the gluon propagator $G(q^2) = G(-q^2)$, the propagator functions S_S obtained in E and ET spaces differ by the phase factor

$$S_s(-p^2) = e^{\pm i\pi/2} S_s(p^2), \quad (3.4)$$

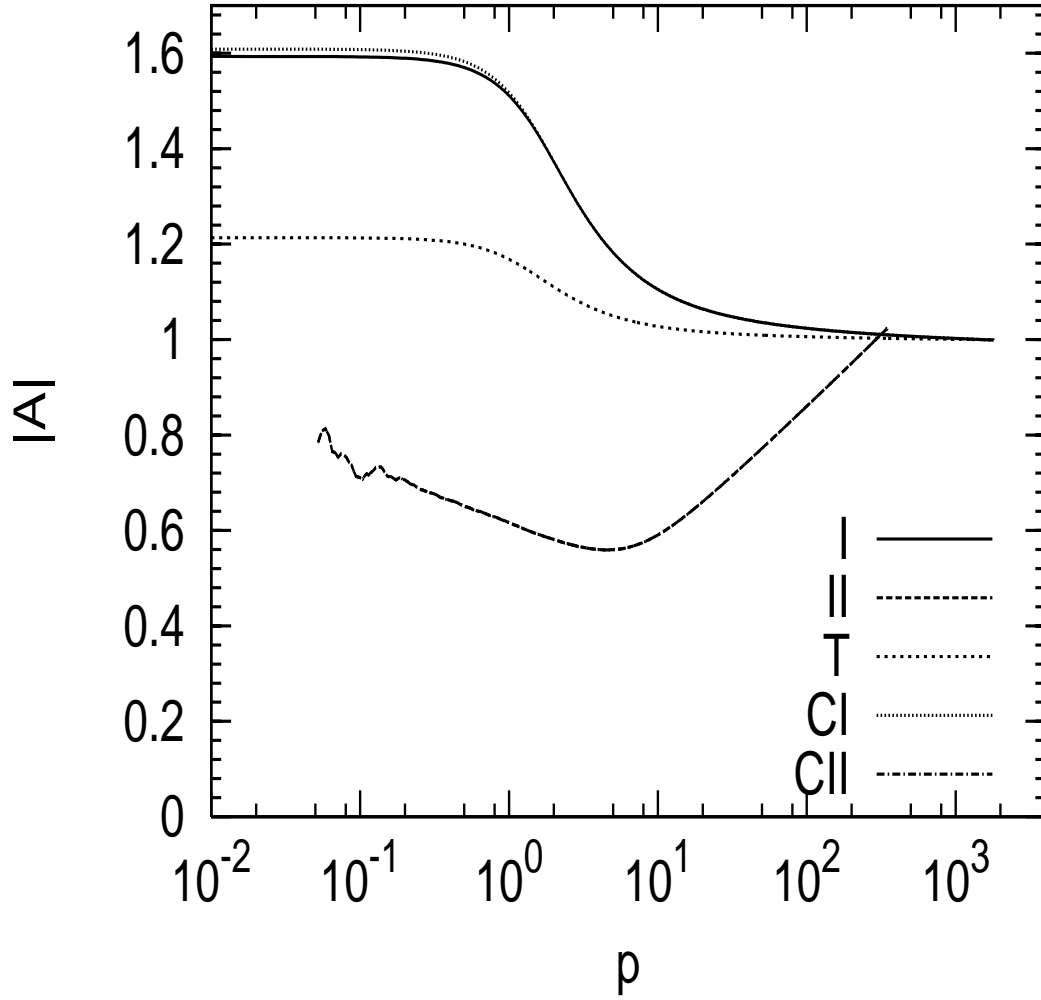


FIG. 4: Renormalization wave functions for the model I and II. The same is shown for the chiral limit (which are indistinguishable in one case). The "Technicolor" T solution is added for for the comparison, the momentum axis is scaled in Λ_{QCD} and Λ_T respectively.

(we use Minkowski space convention in this expression) while the the functions S_V 's are identical in both spaces.

The gap equations above are displayed for small $\beta = 1/2$ and we confirm the solution numerically for any *beta*, i.e. the symmetry is kept for for increasing β , when we are gradually leaving the critical point and reaching the value typical for QCD. No other solution was observed numerically for purely dynamical CSB. We observed that the non zero real imaginary parts of B and A are generated because of nonzero current quark masses, therefore the observed identity (3.1) are only approximate there in the infrared. In reality, the full gluon propagator and the quark-gluon vertex are not suppose to be a simple real and even functions of momenta, but we expect substantial changes due to this. We argue here, solutions of quark gap equations for small current masses already presented in the vast amount of the literature are not only Euclidean solutions usually identified with spacelike Minkowski solution, but up to the phase, they represent a rough but reliable approximation of the timelike Minkowski solution as well.

Although we assume here, the observed structure is crucial for selfconsistent determination of the Greens function in ET space, the resulting phases become irrelevant whenever observables are composed, since the scalar product made from a given amplitude and its conjugated can only represents a measurable quantity.

IV. SUMMARY AND CONCLUSIONS

The first analysis of the light quark gap equations in the Temporal Euclidean space was presented in the paper. We assume that ET solutions represent Minkowski solutions at timelike axis as good as the standard Euclidean solutions the Minkowski spacelike one. Behaviour of the solutions were discussed, the main feature of the all solutions is that the quark mass function is predominantly imaginary, providing confining solution for the quark propagator; such quark propagator has no pole nor branch point at real p^2 axis.

In perturbative QCD and in weak coupling theories generally, the well known calculational trick- the Wick rotation- is under good control. It is a text book knowledge that timelike solution could be obtainable by an analytical continuation of the result conveniently defined and calculated in spacetime Euclidean space. Here, we have assumed no poles and no cuts at a real axis and got complex solution justifying our assumptions. The observed CSB solution in ET space cannot be obtained by analytical continuation of the Euclidean one, it basically differs by the phase. The meaning of that requires more deep understanding.

Recently we do not know how to judge and evaluate the quality of an assumptions we made when switching between Minkowski and Euclidean worlds. The all complex space of four momenta is not under easy control. On the other side, the Euclidean metric simplifies things, how well it approximates our real Minkowski world can be judge a posteriori: The hadrons properties calculated from the QCD Green's functions are recent (future) prospectors of quality of Euclidean (Temporal Euclidean) calculations.

Some possible doubt can follow from unknown prescription of the kernel of considered SDE here. The gluon SDE and related vertices require future selfconsistent analyzes in ET space. It will be certainly more evolving but similar task as the one performed here for the quark gap equation alone. On the other side, we do not think that the improvement towards the exact knowledge of the SDE kernel can drastically change qualitative result. The observed complexification phenomena is very universal as it has happened to two quite different models. However, going beyond the rainbow ladder is task for future Temporal Euclidean space study.

At last but not at least the dynamical CSB has been studied near the critical coupling. The observed numerical solutions obtained do not suggest separation of the dynamical CSB from confinement. These phenomena go hand by hand in hypothetical Walking Technicolors models.

-
- [1] Wilson, Phys. Rev. D10, 2445 (1974)
 - [2] S. Mandelstam, Phys. Lett. B 53, 476, (1975).
 - [3] S. Mandelstam, Phys. Rept. 23, 245, (1976).
 - [4] A. M. Polyakov, Nucl. Phys. B120, 429, (1977).
 - [5] Gerard 't Hooft, Nucl. Phys. B 138, 1, (1978).
 - [6] J. M. Cornwall, Phys. Rev. D22, 1452, (1980).
 - [7] T. Suzuki, I. Yotsuyanagi, Phys. Rev. D42, 4257, (1990).
 - [8] R. Alkofer, J. Greensite, J. Phys. G34, S3, (2007).
 - [9] P. O. Bowman, Kurt Langfeld, D. B. Leinweber, A. O' Cais, A. Sternbeck, L. Smekal, A. G. Williams, Phys. Rev. D78, 054509, (2008).
 - [10] G. S. Bali, Phys. Rev. D62, 114503 (2000).
 - [11] C. D. Roberts and A. G. Williams, Prog. Part. Nucl. Phys. 33, 447 (1994).
 - [12] P. Maris, C.D. Roberts, Int. J. Mod. Phys. E12, 297 (2003).
 - [13] R. Alkofer, L. Smekal, Phys. Rept. 353, 281, (2001).
 - [14] D. Binosi, J. Papavassiliou, JHEP0811:063,2008
 - [15] V. Sauli, Few Body Syst. 39, 45, (2006).
 - [16] J. M. Cornwall, Phys. Rev. D26, 1453, (1982)
 - [17] V. Sauli, J. Adam, Jr., P. Bicudo Phys. Rev. D75, 087701, (2007).
 - [18] V. Sauli, Z. Batiz, J. Phys. G: Nucl. Part. Phys. 36,035002 (2009).
 - [19] V. Sauli, Z. Batiz, arXiv:0901.0110.
 - [20] see any standard textbook on QFT, original paper: G. C. Wick, Phys. Rew. 96, 1124 (1954).
 - [21] J.M. Cornwall, Phys. Rev. D22, 1452 (1980).
 - [22] V.S. Gogoghia, B. A. Magradze, Phys. Lett. B217, 162 (1989).
 - [23] V.N. Gribov, *Possible solution of the problem of quark confinement*, unpublished, U. of Lund preprint LU TP 91-7.
 - [24] C.D. Roberts, A.G. Wiliams, G. Krein, Int. J. Mod. Phys. A, 5607 (1992).
 - [25] D. Binosi, J. Papavassiliou, Phys. Rev. D66, 111901 (2002).
 - [26] A. C. Aguilar, D. Binosi, J. Papavassiliou, Phys. Rev. D78, 025010, (2008).
 - [27] J. M. Cornwall, arXiv:0812.0359 Talk presented at Approaches to QCD, Oberwoelz, Austria, Sept. 2008.
 - [28] $M \pm$ solutions are already observed in standard Euclidean space, L. Chang, Yu-Xin Liu, M. S. Bhagwat, C. D. Roberts, S. V. Wright, Phys. Rev. C75, 015201, (2007).

- [29] P. Maris, Phys. Rev. **D52**, 6087 (1995).
- [30] W. E. Caswell, Phys. Rev. Lett. **33**, 244 (1974).
- [31] T. Banks, A. Zaks, Nucl. Phys. **B196**, 189 (1982).
- [32] F. Sannino, Conformal Windows of $SP(2N)$ and $SO(N)$ Gauge Theories, arXiv:0902.3494.
- [33] B. Holdom, Phys. Rev. D **24**, 1441 (1981).
- [34] T. Appelquist, D. Karabali, and L.C.R. Wijewardhana, Phys. Rev. Lett. **57**, 957 (1986).
- [35] T. Akiba and T. Yanagida, Phys. Lett. **169B**, 432 (1986).
- [36] T. Appelquist, A. Ratnaweera, J. Terning, L. C. R. Wijewardhana, Phys. Rev. **D58**, 105017 (1998).
- [37] T. Appelquist, S. B. Selipsky, Phys. Lett. **B400**, 364 (1997).
- [38] H. Gies, J. Jaeckel, Eur. Phys. J. **C46**, 433 (2006)
- [39] M. Kurachi, R. Shrock, JHEP 0612, 034, (2006).
- [40] T. Appelquist, G. T. Fleming, E. T. Neil Phys. Rev. Lett. **100**, 171607 (2008).
- [41] A. Deuzeman, E. Pallante, M.P. Lombardo, Talk at XXVI International Symposium on Lattice Field Theory, 2008, Virginia, USA, arXiv:hep-lat/08101719.